BAMS Article

ADABBOY

African Dust And Biomass Burning Over Yucatan

Graciela B. Raga, Luis A. Ladino, Darrel Baumgardner, Carolina Ramirez-Romero, Fernanda Córdoba, Harry Alvarez-Ospina, Daniel Rosas, Talib Amador, Javier Miranda, Irma Rosas, Alejandro Jaramillo, Jacqueline Yakobi-Hancock, Jong Sung Kim, Leticia Martínez, Eva Salinas, and Bernardo Figueroa

ABSTRACT: Biomass burning (BB) emissions and African dust (AD) are often associated with poor regional air quality, particularly in the tropics. The Yucatan Peninsula is a fairly pristine site due to predominant trade winds, but occasionally BB and AD plumes severely degrade its air quality. The African Dust And Biomass Burning Over Yucatan (ADABBOY) project (January 2017–August 2018) was conducted in the Yucatan Peninsula to characterize physical and biological properties of particulate pollution at remote seaside and urban sites. The 18-month-long project quantified the large interannual variability in frequency and spatial extent of BB and AD plumes. Remote and urban sites experienced air quality degradation under the influence of these plumes, with up to 200% and 300% increases in coarse particle mass under BB and AD influence, respectively. ADABBOY is the first project to systematically characterize elemental composition of airborne particles as a function of these sources and identify bioaerosol over Yucatan. Bacteria, actinobacteria (both continental and marine), and fungi propagules vary seasonally and interannually and revealed the presence of very different species and genera associated with different sources. A novel contribution of ADABBOY was the determination of the ice-nucleating abilities of particles emitted by different sources within an undersampled region of the world. BB particles were found to be inefficient ice-nucleating particles at temperatures warmer than –20°C, whereas both AD and background marine aerosol activated ice-nucleating particles below –10°C.

KEYWORDS: Air pollution; Biomass burning; Dust or dust storms; Ice particles; Tropics; Wildfires

https://doi.org/10.1175/BAMS-D-20-0172.1
Corresponding author: Darrel Baumgardner, darrel.baumgardner@gmail.com
In final form 30 March 2021

AFFILIATIONS: Raga, Ladino, Ramirez-Romero, Córdoba, Rosas, Jaramillo, Martínez, and Salinas—Centro de Ciencias de la Atmósfera, Universidad Nacional Autónoma de México, Mexico City, Mexico; **Baumgardner**—Droplet Measurement Technologies, LLC, Longmont, Colorado; **Alvarez-Ospina**—Facultad de Ciencias, Universidad Nacional Autónoma de México, Mexico City, Mexico; **Rosas and Amador**—Facultad de Química, Universidad Autónoma de Yucatán, Mérida, Yucatán, Mexico; **Miranda**—Instituto de Física, Universidad Nacional Autónoma de México, Mexico City, Mexico; **Yakobi-Hancock and Kim**—Dalhousie University, Halifax, Nova Scotia, Canada; **Figueroa**—Instituto de Ingeniería, Unidad Académica de Sisal, Universidad Nacional Autónoma de México, Sisal, Yucatán, Mexico

Mineral dust particles and marine salts globally constitute the most abundant natural aerosols in the atmosphere (Andreae 1995). Other natural sources, e.g., vegetation and microorganisms, emit substantial quantities of primary biological aerosol (Despreìs et al. 2012) and precursor gaseous species resulting in secondary aerosol formation (Chen et al. 2009). Particles affect the radiation budget of the Earth (Forster et al. 2007) and impact the local and regional hydrological cycle as cloud condensation nuclei (CCN) (Lau and Wu 2003; Zhang et al. 2007; Raga et al. 2016; Liu et al. 2018) and ice-nucleating particles (INPs) (Creamean et al. 2013; Yakobi-Hancock et al. 2014; Wilson et al. 2015; Kanji et al. 2017).

Biomass burning (BB) encompasses wildfires, forest/savannah clearance for agriculture, removal of agricultural residue, and domestic cooking/heating. BB emissions constitute a health threat (Wiedinmyer et al. 2006). Anthropogenic BB is prevalent in tropical regions and exhibits a clear peak during the dry season (Giglio et al. 2006; Giglio 2007). BB emissions affect the regional radiative budget, increasing atmospheric stability and inhibited convection (Koren et al. 2004; Feingold et al. 2005). While most of the aerosol emitted from BB impacts local and regional areas, under particular weather patterns BB plumes are advected over thousands of kilometers. Aerosol plumes emitted by BB in southern Mexico and Central America have impacted urban air quality in the United States (Peppler et al. 1999; van der Werf et al. 2006; Dominguez-Martinez and Rodriguez, 2008; Yokelson et al. 2009, 2011). Some BB particles are active as CCN (Rogers et al. 1991), but it is still unclear under which conditions BB particles are efficient INPs (Kanji et al. 2017).

African dust (AD) increases atmospheric particulate mass (PM) significantly affecting most of the countries surrounding the Mediterranean Sea (Ganor and Mamane 1982; Guerzoni et al. 1997) and the tropical Atlantic Ocean (Mukhopadhyay and Kreycik 2008; Evan and Mukhopadhyay 2010). Annual AD episodes affect the tropical Atlantic that degrades air quality in Barbados and Miami during boreal summers (Prospero and Mayol-Bracero 2013). AD originating in deserts located between 15° and 25°N travels over the Atlantic in an elevated layer (the Saharan aerosol layer, SAL), reported originally by Carlson and Prospero (1972) and Prospero and Carson (1972). This warm and dry air mass laden with dust particles travels westward at a speed of about 1,000 km day^{-1}, reaching Barbados in the Lesser Antilles in ~5 days. The SAL exhibits large seasonal variability (Huang et al. 2010), and is transported primarily into the Caribbean and Florida in June and July (Weinzierl et al. 2017). Aircraft and shipborne measurements during the Saharan Aerosol Long-Range Transport and Aerosol–Cloud–Interaction Experiment (SALTRACE) (Weinzierl et al. 2017) characterized the plume as it leaves Africa (Cape Verde) and upon reaching Barbados. Airborne lidar observations show that the SAL over Cape Verde extends from a base at 1.5 km above the cool and dust-free trade winds to a top around 6–7 km. As the SAL progresses westward, its depth decreases to ~4 km above Barbados as it reaches the surface. The trade wind inversion weakens westward, favoring entrainment of the overlaying dust and mixing throughout the boundary layer, where turbulence and aerosol–cloud interactions affect

dust concentration. A similarly detailed picture has yet to emerge to describe the vertical structure and evolution of the SAL as it continues westward over the Caribbean Sea. Prospero and Mayol-Bracero (2013) recommended the expansion of AD monitoring throughout the Caribbean; thus, our research group implemented a field project to document the arrival of dust plumes in Mexico.

The Yucatan Peninsula, in southeastern Mexico surrounded by the Caribbean Sea and the Gulf of Mexico, is home to sensitive ecosystems and invaluable archeological sites (Fig. 1). Agricultural lands dominate with only a few small- and medium-sized cities, such as Merida and Cancun with ~890,000 and 740,000 inhabitants (INEGI 2015). Yucatan was selected for this study because its relatively clean air, due to predominant trade winds, is significantly perturbed during periods of BB in southern Mexico and Central America and during occasional incursions of AD.

Scientists from the National University of Mexico (UNAM), the University of Yucatan (UADY), and Dalhousie University in Canada conducted the African Dust And Biomass Burning Over Yucatan (ADABBOY) project from January 2017 to August 2018, with continuous measurements supplemented by six intensive observation periods (IOPs).

ADABBOY's primary goal was to identify main sources of particles affecting Yucatan, focusing on BB, AD, marine, and biological particles, and establishing a baseline of background conditions for future studies. Specific objectives were to

- identify and characterize background, BB and AD particles;
- quantify the influence of BB and AD particles on urban air quality;
- document biological microorganisms in BB and AD plumes; and
- locate the main sources of INPs and quantify the ice-nucleating abilities of marine, BB, and AD particles.

ADABBOY campaigns

The Yucatan Peninsula (Fig. 1) is a flat limestone terrace with a warm, semidry climate on the Gulf of Mexico coast and a warm, subhumid climate throughout the rest of the region. In situ measurements were made in Merida (20.9754°N, 89.6170°W), located ~23 km from the coastline, and in the coastal village of Sisal (21.1653°N, 90.0311°W). Merida is rapidly growing due to tourism and the relocation of industries from within Mexico. Sisal, a fishing village (population 1,837; SEDESOL 2013), enjoys clean air, with the closest

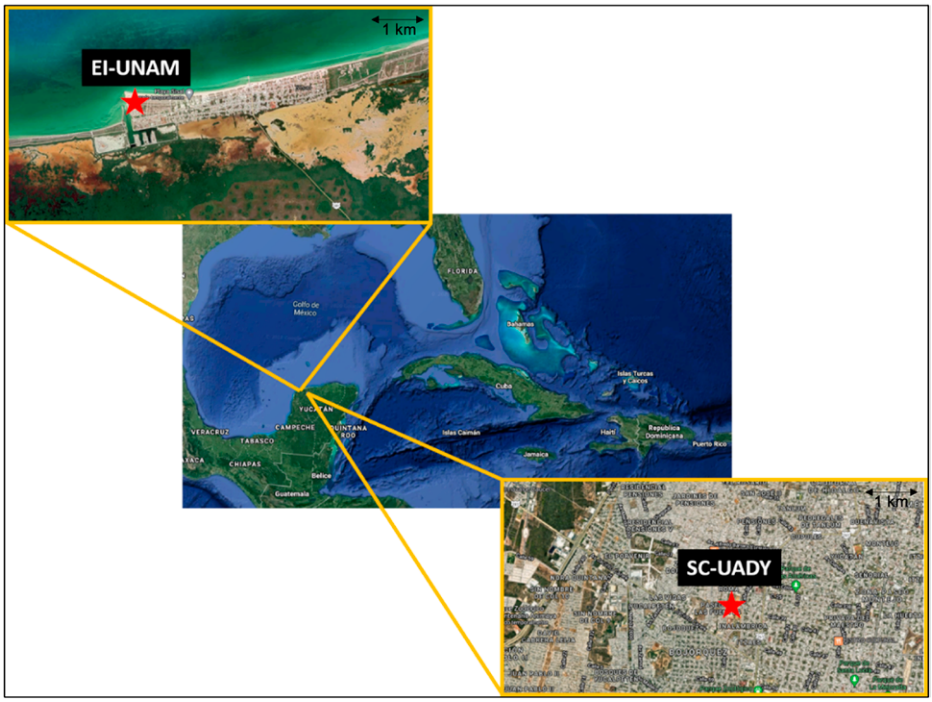

Fig. 1. Sampling sites in the Yucatan Peninsula: Merida (urban; 20.9754°N, 89.6170°W) and Sisal (remote seaside; 21.1653°N, 90.0311°W), Mexico. EI-UNAM and SC-UADY refer to the Engineering Institute of the National University of México and the School of Chemistry of the University of Yucatán, respectively (map source: Google Maps).

source of industrial emissions located ~25 km inland and the closest city, Merida, ~50 km away.

Airborne particles were continuously monitored at the School of Chemistry at UADY, located in the central-western part of Merida (inset, Fig. 1). Table 1 lists the instrumentation used to characterize particle properties. Six IOPs complemented the continuous measurements: four in Merida (April 2017, July 2017, April 2018, and July 2018) and two in Sisal (January 2017 and July 2018). Documentation of the seasonality of BB and AD events in Yucatan was used to select optimal periods for the IOPs, as discussed further below.

Elemental composition from filter samples determined by X-ray fluorescence (Espinosa et al. 2012) provide in situ confirmation of aerosol categories. Rodríguez-Gómez et al. (2020) discuss the sampling methodology for microorganisms, while Córdoba et al. (2021) and Ladino et al. (2021) document ice-nucleating properties of aerosol and seawater samples.

Climatological context and previous studies. The Yucatan Peninsula is characterized by a dry season (December–May) and a rainy season (June–November) punctuated by intense cold fronts during December–February.

Table 1. List of the instrumentation deployed in the measurement site in Merida (located at 12 m above ground level) and the institution that provided them.

Instrument	Variable	Institution[a]
Meteorological station (HMP 155, Vaisala)	*T*, RH, wind speed, wind direction, precipitation, and solar radiation	RUOA, UADY
Continuous ozone analyzer (model 49i, Thermo Scientific, Inc.)	Mixing ratio of O_3	RUOA, UADY
Continuous nitrogen oxides analyzer (model 42i, Thermo Scientific, Inc.)	Mixing ratio of NO and NO_2	RUOA, UADY
Continuous sulfur dioxide analyzer (model 43i, Thermo Scientific, Inc.)	Mixing ratio of SO_2	RUOA, UADY
Continuous carbon monoxide analyzer (model 48i, Thermo Scientific, Inc.)	Mixing ratio of CO	RUOA, UADY
Continuous particulate monitor via beta attenuation (FH 62 C14, Thermo Scientific, Inc.) with PM_{10} inlet	Particulate matter mass of particles with sizes below 10 μm	RUOA, UADY
Continuous particulate monitor via beta attenuation (FH 62 C14, Thermo Scientific, Inc.) with $PM_{2.5}$ inlet	Particulate matter mass of particles with sizes below 2.5 μm	RUOA, UADY
Photoacoustic Extinctiometer, PAX (Droplet Measurement Technologies, Inc., USA)	Optical aerosol properties and equivalent black carbon (derived)	RAMA
8stage Micro-orifice uniform deposit impactor (MOUDI 100R and 100NR, MSP) ×2[b]	Collection of aerosol (by size) particles for chemical analysis and ice nucleation analysis	AA-CCA IMM-CCA
Mini-Vol sampler (3380, Air metrics) and (TAS, Air metrics) ×3[b]	Collection of aerosol particles ($PM_{2.5}$ and PM_{10}) for chemical analysis	AA-CCA IMM-CCA
Biostage Impactor (Quick Take 30, SKC, Inc. USA) ×2[b]	Collection of aerosol particles for detection of biological particles	Ab-CCA IMM-CCA
Condensation particle counter (3010, TSI) ×2[b]	Concentration of aerosol particles larger than 50 nm	IMM-CCA
Optical particle counter (LasAir, 310A, PMS) ×2 and (LasAir 310C, PMS)[b]	Size distribution of aerosol particles larger than 300 nm	IMM-CCA
Ice-nucleating particle counter, UNAM- MOUDI-DFT	Concentration of ice-nucleating particles	IMM-CCA
Droplet freezing assay, UNAM-DFA	Concentration of ice-nucleating particles	IMM-CCA
Particle soot absorption photometer, (PSAP Radiance Research)	Aerosol absorption coefficient	IMM-CCA
Photoelectric aerosol sensor (PAS, 2000, EcoChem)	Polycyclic aromatic hydrocarbons concentration	IMM-CCA
Partisol (2525, Thermo Fisher Scientific, Inc.)	Collection of aerosol particles for chemical analysis	DU
Ultrafine particle monitor (3031, TSI, Inc.)	Size distribution of fine and ultrafine particles (20–200 nm)	DU

[a] ROUA: UNAM's Network of Atmospheric Observatories; UADY: University of Yucatan; CCA: Center from Atmospheric Sciences at UNAM; DU: Dalhousie University; RAMA: Automatic Monitoring Network, Mexico City. Three groups from CCA-UNAM contributed instrumentation: Micro-Mesoscale Interactions (IMM); Aerobiology (Ab), and Atmospheric Aerosols (AA).

[b] This equipment was deployed in Sisal during the intensive observation periods during ADABBOY.

Dry-season BB activities peak between March and May (Rios and Raga 2018, 2019; Trujano-Jiménez et al. 2021), so IOPs were carried out in April 2017 and 2018 to maximize the chances of sampling BB particles. Real-time satellite information, forecast aerosol plumes (e.g., www.nrlmry.navy.mil/aerosol/) and HYSPLIT back trajectories confirmed the origin of the BB emissions.

Easterly waves and tropical cyclones affect the region during the rainy season, with rainfall modulated intraseasonally by the Madden–Julian oscillation (MJO) and interannually by El Niño–Southern Oscillation (ENSO). A relative minimum in precipitation is observed in July–August, known as the "midsummer drought," which is associated with a strengthening of the Caribbean low-level jet accompanied by decreased probability of tropical cyclone landfall over Yucatan (Magaña et al. 1999; Karnauskas et al. 2013; Diaz-Esteban and Raga 2017; Perdigón-Morales et al. 2019).

The Modern-Era Retrospective Analysis for Research and Applications, version 2 (MERRA-2), is used to estimate a 17-yr climatology of the dust component of PM_{10}. Figure 2 shows that during July the largest mean concentrations are over the eastern Atlantic and that values near Yucatan are higher than over Cuba and southern Florida. Thus, IOPs were conducted in July 2017 and July 2018 to maximize the chance of sampling AD plumes.

Few studies have quantified the presence of BB plumes in Yucatan. Korontzi et al. (2006) analyzed 3 years of MODIS data and Yokelson et al. (2011) reported evidence of smoke from fires over Yucatan obtained from aircraft measurements during the MILAGRO campaign. Rios and Raga (2018, 2019) provide a 14-yr climatology of

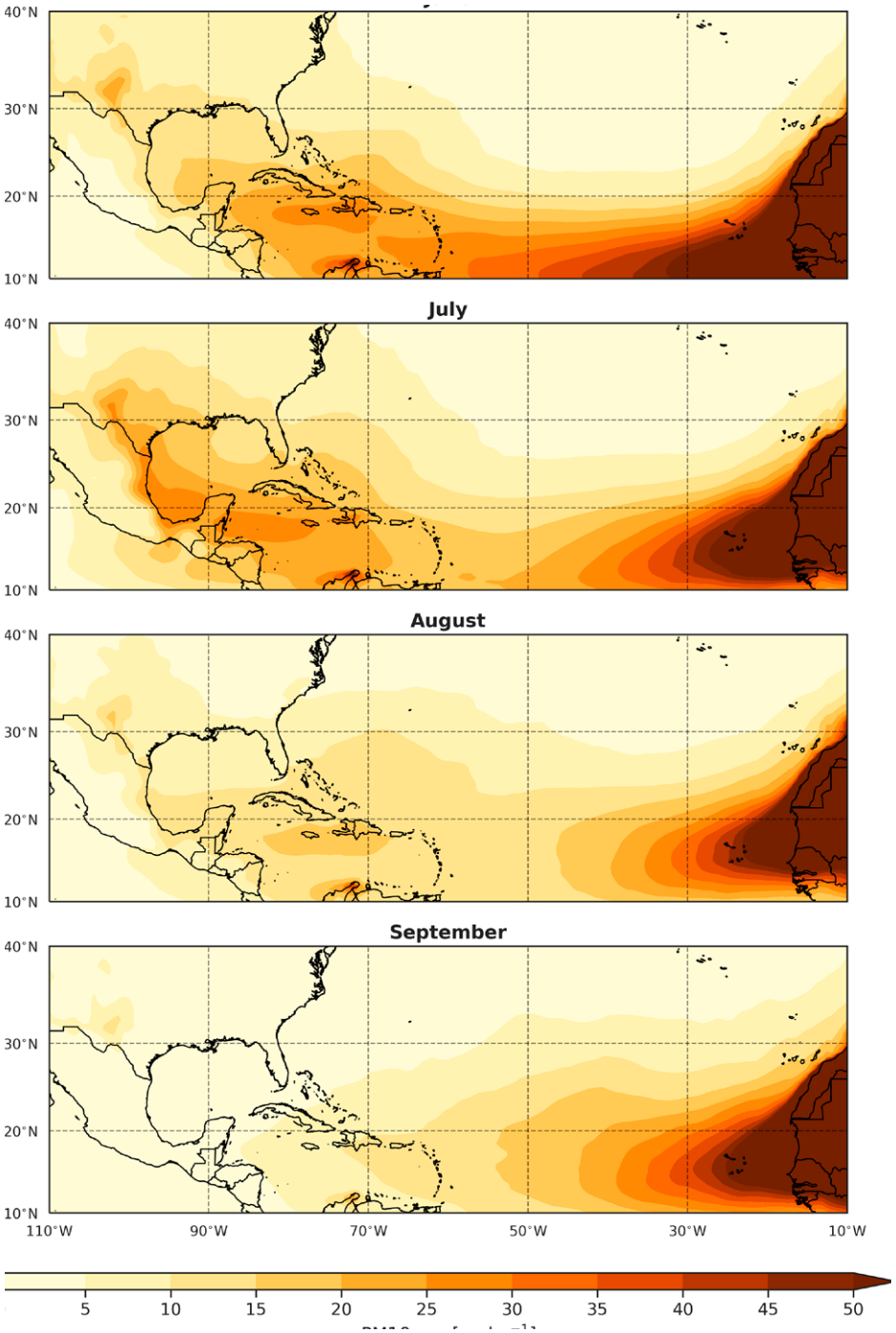

Fig. 2. Mean monthly PM_{10} concentration associated with dust derived from MERRA-2 over 2003–19, for June–September. The two sampling sites are represented by a single black dot due to their proximity.

burned areas in tropical forests and agricultural lands, estimating their emissions and interannual variability and showing that BB activities peak during March–May. However, the properties of particulate BB emissions have not been systematically studied before.

Even less research has identified the potential presence of AD in the Yucatan Peninsula. Satellite lidar observations (Adams et al. 2012) suggested that during June–August AD particles reach Yucatan within the boundary layer, between the surface and 2 km. Das et al. (2013), from a few surface samples at a single inland location, suggested that phosphorus in the soil was potentially associated with dry and/or wet deposition of AD. Given the paucity of observations in this region, ADABBOY provides valuable, in situ data on the arrival of AD plumes over northern Yucatan.

Aerosol particle characterization.

Physical properties Annual average $PM_{2.5}$ and PM_{10} concentrations in Merida for 2016–18 are less than 9.7 and 24 μg m^{-3}, respectively, close to the 10 and 20 μg m^{-3} recommended by the World Health Organization (Ramírez-Romero et al. 2021; Muñoz-Salazar et al. 2020). Average background number concentrations for particles >30 nm are <3000 cm^{-3} in Sisal and Merida (Muñoz-Salazar et al. 2020) and are significantly reduced upon the arrival of cold fronts (Ladino et al. 2019). Episodes of greatly enhanced concentrations (up to 55,000 cm^{-3}) of ultrafine particles (20–200 nm) were observed in Merida, likely associated with new particle formation triggered by photochemistry (Muñoz-Salazar et al. 2020).

AD and BB aerosol plumes are sporadic events, lasting 1–3 days per event, and exhibit large interannual variability. During ADABBOY there were four AD and seven BB events in 2017 and six AD and four BB events in 2018. PM_{10} in Merida increases significantly when AD plumes arrive, at times more than 300% above background (Ramírez-Romero et al. 2021). The PM_{10} 24-h average observed during AD individual events in 2018 reached ~38 μg m^{-3}, not exceeding the WHO guideline of 50 μg m^{-3}. Hourly values can be much higher, such as the "giant" AD event from 23 to 27 June 2020 when PM_{10} values reached as high as 317 μg m^{-3} (Mayol-Bracero et al. 2020). PM_{10} influenced by BB increases by as much as 200% above background (Ramírez-Romero 2019). These events deteriorate air quality but the interannual variability in duration and intensity modulates their health and environmental impacts.

The increase in total number concentration under BB and AD conditions is the result of large changes in number and volume particle size distributions. Neither BB nor AD plumes represent near-source, fresh emissions and the distributions have experienced processing in the atmosphere while advected into Yucatan. The number size distribution (Fig. 3a) shows that particles sampled during AD episodes dominate in the size range 0.05–0.3 μm, while BB-influenced are comparable to background. Since the size intervals increase with size, the size distributions are normalized by dividing the number or volume concentration in each size interval by the logarithm of that interval. The large concentration of small particles observed during AD is consistent with measurements made by aircraft near Cape Verde in 2015 (Liu et al. 2018); smaller AD particles with lower sedimentation rates are more likely to reach Yucatan. AD particles have larger concentrations than the background in all size ranges, but BB particles exceed AD concentrations for sizes above 0.3 μm. This is also evident in the volume size distributions (Fig. 3b) in which AD shows a bimodal distribution of comparable concentration, while BB volume dominates the size range from 1 to 5 μm. Volume size distributions are related to mass, assuming a nominal density for each aerosol type (MA, BB, or AD). Selected statistics are summarized in Table 2.

Chemical properties. The percentage elemental composition of particles under background conditions, i.e., under no influence of either BB or AD plumes, are shown for Merida (Fig. 4a) and Sisal (Fig. 4b). Sodium (Na) and chlorine (Cl) are ubiquitous due to proximity to the Gulf

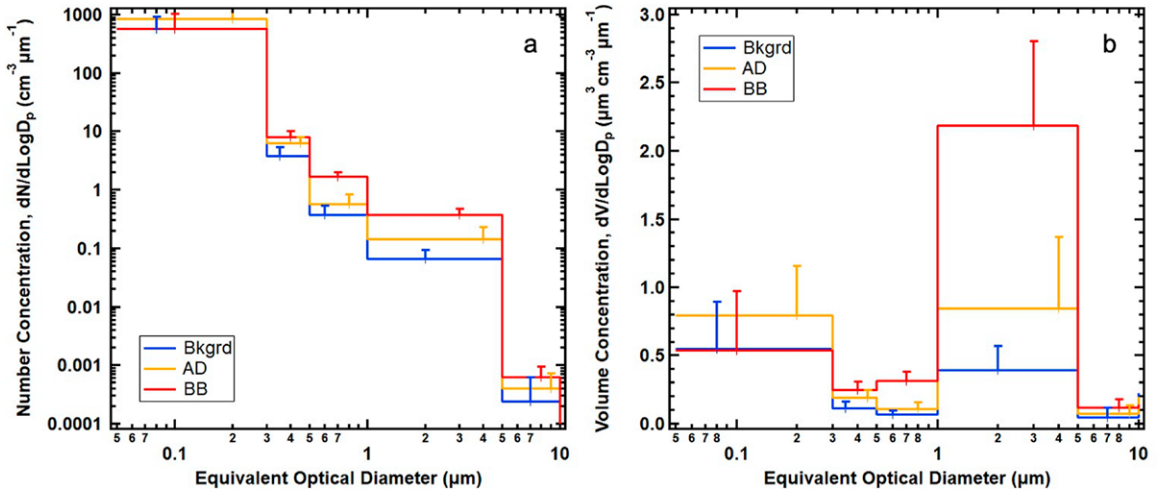

Fig. 3. Particle (a) number and (b) volume concentrations as a function of equivalent optical diameter (EOD) for particles larger than 50 nm stratified by air masses, normalized by the logarithm of the channel size intervals. The distributions are the result of combining measurements from the PMS LasAir with those from the TSI CPC. The volume distributions are computed assuming particle sphericity at the EOD. The sizing uncertainty is on the order of ±20%. The AD distributions (yellow) and the BB distributions (red) were obtained from selected individual plumes that affected Merida. The average background distribution (blue) was obtained from samples not affected by AD or BB in Merida. Vertical error bars indicate one standard deviation and are only shown in the postive direction for clarity.

of Mexico and Caribbean Sea (Córdoba et al. 2021). Calcium (Ca) is also part of the background composition since Cretaceous sediments form the Yucatan soil. Sulfur (S) observed in Sisal (Fig. 4b) is likely the result of dimethyl sulfide (DMS) emissions by phytoplankton; in fact, January samples in Sisal for marine background indicate that non-sea-salt sulfate makes up more than 50% of the composition (Córdoba 2019). Urban emissions in Merida modify the background composition indicating more S, associated with diesel fuel combustion for power generation and transport (Fig. 4a). Na, Cl, S, and Ca account for more than 70% of the composition of background samples.

The elemental composition of BB particles depends on the type of fuel burned (Akagi et al. 2011). The red bars in Fig. 4c show the enrichment factor for each element associated with BB emissions, relative to the background samples in Merida. Such samples indicate the expected enrichment of potassium (K), a key plant nutrient released during the combustion of vegetation (Ackerman and Cicek 2017). There is good correlation between the time series of $PM_{2.5}$ and K for the BB periods. (Pearson correlation coefficient, $CC_P = 0.6$). Analysis also indicates increased S associated with BB. A large fraction of BB particle composition would be carbonaceous so selected samples from 2017 in Merida were analyzed for total carbon (TC

Table 2. Statistics derived from the number and volume concentration distributions from samples affected by BB and AD compared to average background samples in Merida (samplers located at 12 m above ground level).

	Number concentration (cm^{-3})			Volume concentration ($\mu m^3\ cm^{-3}$)		
	Median	75th percentile	90th percentile	Median	75th percentile	90th percentile
Background	450	750	1030	0.160	0.255	0.290
BB	480	680	890	0.280	0.365	0.430
AD	700	1060	1400	0.255	0.350	0.450

=organic + elemental). A significant increase in TC (by ~70%–80%) is seen in samples of BB versus AD (Córdoba et al. 2021). Elemental components associated with fossil fuel combustion in Merida do not exhibit seasonality, so the difference in TC between BB and AD samples is directly linked to differences in organic carbon, as would be expected from the combustion of vegetation.

The elemental composition of AD has been studied utilizing different methodologies and distances from the sources, e.g., near sources in Africa and downwind over Cape Verde (e.g., Kandler et al. 2011; Bozlaker at al., 2018; Liu et al. 2018), Barbados (Trapp et al. 2010; Kandler et al. 2018), Miami (Prospero et al. 2010), and the Gulf Coast of Texas (Bozlaker et al. 2019). The arrival of AD over Yucatan in July is marked by the large increase in aluminum (Al), silicon (Si), and iron (Fe) as seen in Fig. 4c (yellow bars), compared to the background composition, and modest enrichment of magnesium (Mg) and titanium (Ti), all key elements in mineral dust (Linke et al. 2006; Marsden et al. 2019; Querol et al. 2019). During the AD period, there is excellent correlation between the time series of $PM_{2.5}$ and Mg (CC_P = 0.82), Al (CC_P = 0.94), Si (CC_P = 0.94), Ti (CC_P = 0.89), and Fe (CC_P = 0.88). Our results are consistent with the AD elemental profile reported by Bozlaker et al. (2018) from samples in Barbados. Moreover, Bozlaker et al. (2019) measured $PM_{2.5}$ in Houston and Galveston, Texas, during an AD event between 17 and 25 August 2014 that led to mass doubling, which is also observed in our study. Enrichments of Mg, Al, Si, Ca, Ti, Mn, and Fe in our samples are consistent with their results.

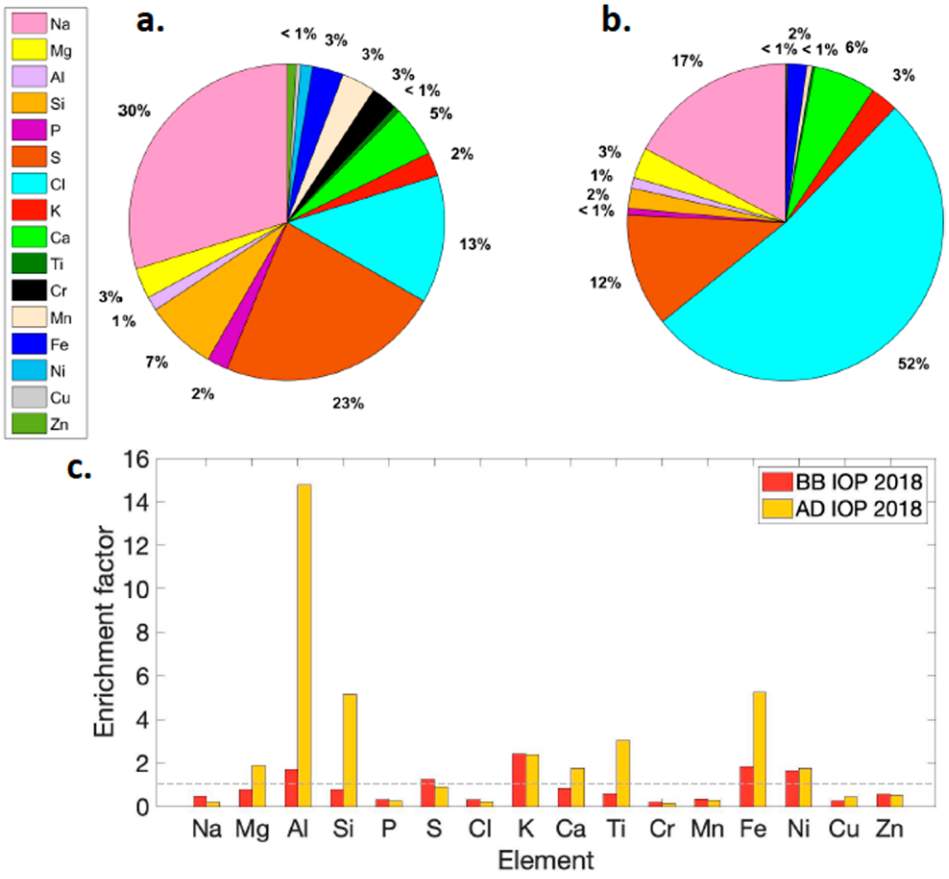

Fig. 4. Percentage elemental mass concentration for background samples in (a) Merida and (b) Sisal. (c) Enrichment factors calculated for samples obtained under the influence of BB (red bars) and AD (yellow bars) plumes with respect to the background conditions sampled in Merida. The dashed horizontal line corresponds to enrichment factor equal to 1.

Biological properties. Maritime and continental microorganisms are ubiquitous in Yucatan since temperature and relative humidity favor their proliferation and survival (Ponce-Caballero et al. 2013). Culturable bacteria, fungal propagules and actinos (marine and continental actinobacteria) were detected during ADABBOY (Rodriguez-Gomez et al. 2020). The concentration of fungal propagules is ~3 times higher than of bacteria, both in Sisal and in Merida (Fig. 5). A threefold to fivefold increase in number concentration of bacteria and fungal propagules is observed between MA and AD, associated with African air masses. Nevertheless, the impact of the local meteorology in the concentration and diversity of bioparticles in the Yucatan Peninsula requires careful evaluation (Rodríguez-Gómez et al. 2020).

While similar bacteria genera were observed during all IOPs, different species were present in MA and AD, e.g., *Vibrio* spp. were identified in samples of MA during cold fronts, typical of marine environments, while *Microbacterium*, *Sphingomonas*, *Bacillus*, and *Streptomyces* were isolated and identified during AD episodes, in agreement with Griffin (2007). *Cladosporium* and *Penicillium* were the dominant fungi under background conditions whereas during the influence of the AD plumes additional genera, such as *Alternaria*, *Fusarium*, and *Tricomona/Monillia*, were identified by Rodriguez-Gomez et al. (2020).

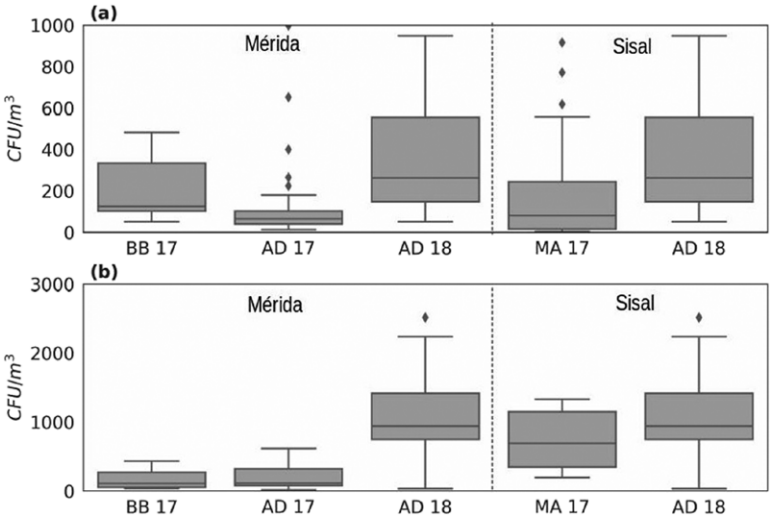

Fig. 5. Boxplots of the concentration [CFU m^{-3}] of (a) bacteria and (b) fungal propagules. BB, AD, and MA refer to biomass burning, African dust, and marine aerosol IOPs during 2017 and 2018. Samples are exposed for 5 min and results are counts after 48 h (modified from Rodriguez-Gomez et al. 2020).

Low concentrations of bacteria and fungal propagules were found during the BB period (Fig. 5), especially for fungal propagules, in agreement with Ponce-Caballero et al. (2013). BB activities in the tropics are dominant during the dry season with relatively lower relative humidity, a factor that limits the production of microorganisms.

ADABBOY highlighted the interannual variability of the AD plumes arriving in the Yucatan Peninsula that impacts the sampled microbiota (Fig. 5: Merida, AD17 vs Merida, AD18), supporting the hypothesis that African plumes may transport foreign microorganisms onto Mexican territory.

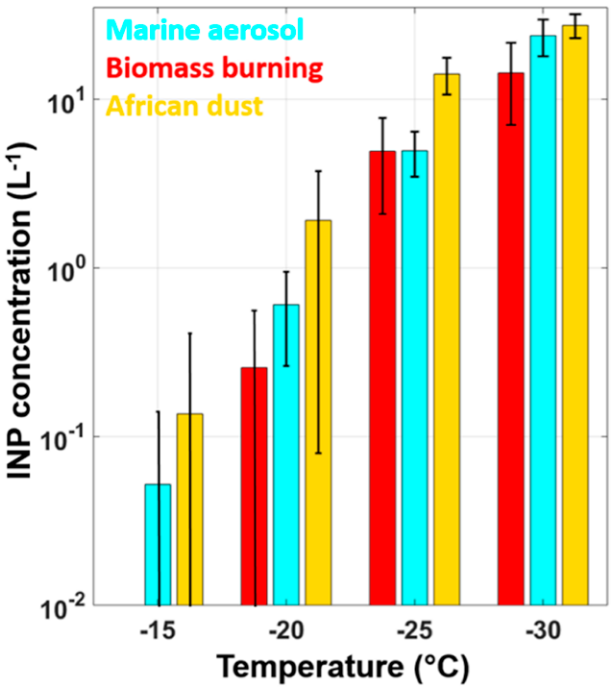

Fig. 6. INP concentration as a function of temperature for three distinct air masses: marine aerosol (MA, blue), biomass burning (BB, red), and African dust (AD, yellow) for particles with sizes ranging between 0.32 and 10 μm. The vertical black lines indicate the standard deviation (modified from Córdoba et al. 2021).

Ice-nucleating properties associated with immersion freezing. Since most of the precipitation over Yucatan forms in deep clouds at temperatures well below 0°C (Diaz-Esteban and Raga 2019) it is relevant to determine the ice-nucleating abilities of MA compared with BB and AD particles. Figure 6 summarizes the INP concentrations as a function of temperature and aerosol type. The BB particles do not activate at temperatures warmer than –15°C, consistent with other studies (Kanji et al. 2017). In contrast, MA and AD are ice active between –15° and 0°C. AD as INP have been extensively studied by airborne sampling in the eastern Atlantic near Africa (e.g., DeMott et al. 2003; Twohy et al. 2009; Price et al. 2018, among many others) and in the laboratory (Augustin-Bauditz et al. 2014; DeMott et al. 2015). At –15°C the AD plumes sampled in Yucatan contained higher INP concentrations than MA. Nevertheless, the most efficient particles were those collected during the passage of cold fronts under predominantly maritime conditions, with onset

freezing temperatures as warm as –3°C (Ladino et al. 2019) and higher active site densities (Córdoba et al. 2021). The activation fraction of most of the AD samples collected in Yucatan are slightly less efficient than airborne filter samples near Cape Verde reported by Price et al. (2018), with AD samples in Yucatan at –20°C about two orders of magnitude less in concentration. Below –20°C the highest INP concentrations were found in AD, followed by MA and BB particles. These results are in excellent agreement with results from other locations as summarized by Kanji et al. (2017). The AD was identified as the main source of INPs in the Yucatan Peninsula during the midsummer season, with a high potential to affect local and regional precipitation. Nevertheless, the MA particles are ubiquitous all year-round, contributing significantly to INPs and precipitation development.

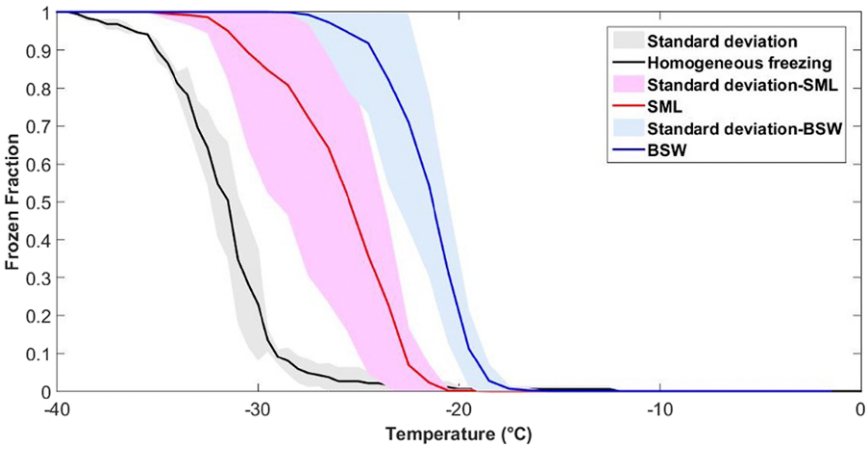

Fig. 7. Frozen fraction curves for the sea surface microlayer (SML, red line) and bulk surface water (BSW, blue line) samples collected at the Gulf of Mexico. The solid black line denotes the homogeneous freezing curve and the shaded areas denote the standard deviation for each sample type (modified from Ladino et al. 2021).

Seawater around Yucatan is a large source of airborne particles, as a result of bubble bursting and wave breaking at the surface, including salts, microorganisms and exudates. Water samples were obtained from the sea surface microlayer (SML) and from the bulk-surface water (BSW) near the Gulf of Mexico coast. The ice-nucleating abilities of water samples from the SML and the BSW were determined using the UNAM-Droplet Freezing Assay. Surface layer waters contain ice active material (Fig. 7), with INP concentrations ranging between 6.0×10^1 and 1.1×10^5 L^{-1} water at temperatures below –16.5°C (Ladino et al. 2021).

Microorganisms are good INPs (Maki and Willoughby 1978; Yankofsky et al. 1981) and airborne microorganisms were sampled and identified during ADABBOY. Analysis of the 13 bacteria species isolated from air samples—firmicutes, actinobacteria, beta-proteobacteria and gamma-proteobacteria phylum—indicate that they are inefficient INPs (onset freezing temperatures < –18°C) compared to other bacteria, such *Pseudomonas syringae* (Yankofsky et al. 1981; Wex et al. 2015).

Summary and outstanding questions

ADABBOY identified sources of aerosol particles in the Yucatan Peninsula, documented their properties, and evaluated the impact on local air quality of regional BB emissions and long-range transport of African dust, sporadic sources with different seasonality, revealing significant differences:

- Under the influence of BB and AD plumes, PM_{10} mass concentrations increase up to 200% and 300% above background, respectively.
- The BB number concentrations are comparable to the background at sizes smaller than 0.3 μm while AD concentrations are a factor of approximately two higher than BB and background in the size range from 0.05 to 0.3 μm.
- BB volume concentrations dominate in the size range 1–5 μm while AD volume size distributions are bimodal.

- Background aerosol composition is dominated by Cl, Na, and S.
- BB particles are enriched in K and S, as well as in total carbon and significantly correlated with $PM_{2.5}$.
- AD particles are highly enriched in Al, Si, Fe, Mg. and Ti and significantly correlated with $PM_{2.5}$.
- *Alternaria*, *Fusarium*, and *Tricomona/Monillia* were identified in AD while *Cladosporium* and *Penicillium* are dominant fungi genera in background.
- BB particles are inefficient INP at temperatures warmer than –20°C whereas both AD and MA are active INP below –10°C.

Data collected during ADABBOY will help constrain models of emission and transport of BB and AD. The temperature dependency of INPs is important for validating current parameterizations of ice crystal formation in tropical regions as a precursor to mixed-phase precipitation in weather and climate models. The broad range of bacteria, fungi, and actinobacteria, known sources of INPs, suggests that they might play a role in cloud formation and precipitation in this region.

This study significantly expands the existing dataset of particle properties in this region and raises several issues to be addressed in future studies:

- Evaluate mitigation measures for anthropogenic BB activities that degrade air quality and threaten sensitive ecosystems in natural protected areas.
- Analyze the interannual variability of AD intrusions related to regional air quality.
- Assess the role of AD related nutrients on biogeochemical processes with expanded sampling of bulk deposition in the Yucatan.
- Evaluate the role of endemic microorganisms versus those transported to Yucatan by cold fronts, tropical cyclones, and AD plumes.
- Evaluate the role of regional phytoplankton blooms as INPs.

ADABBOY has documented the near-pristine environment that is polluted yearly by emissions from BB and AD intrusions. BB is an anthropogenic activity that can and should be mitigated in the future. AD events may increase as climate changes and desertification in Africa expands (Liu and Xue 2020). Given that Yucatan is representative of much of the western Caribbean and Central America, in that BB is a common practice and AD also reaches those other areas, long-term monitoring at one or more sites in the region will provide in situ evidence of the future evolution of BB and AD. This first detailed study of particle properties in this region provides a valuable baseline for future studies.

Acknowledgments. ADABBOY was supported by a large number of students that contributed valuable time and effort towards their undergraduate and graduate-level theses, contributing to publications cited. We hereby explicitly acknowledge the important contributions of Manuel Andino, Diego Cabrera, Aline Cruz, Sofia Giordano, Javier Juarez, Aimee Melchum, Joshua Muñoz, Diana Pereira, Zyanya Ramírez, and Camila Rodríguez. The authors also thank to Allan Bertram, Elizabeth García, Gabriel García, Manuel García, Victor García, Wilfrido Gutiérrez (deceased), Jorge Herrera, Lisa Miller, Juan Carlos Pineda, Rosario Pool Chi, Miguel Robles, Alfredo Rodríguez, and Ma. Isabel Saavedra. Funding was provided by Conacyt (FC-2164 and SNI-I1200/16/2019), PAPIIT-UNAM (IN102818, IA108417, and IN111120), RUOA-UNAM, and UADY (SISPROY-FQUI-2018.0003). NASA and NOAA are acknowledged for making MODIS data, MERRA-2 data, and HYSPLIT available.

Data availability statement. The ADABBOY dataset is available upon request to L.A. Ladino (luis.ladino@atmosfera.unam.mx).

References

Ackerman, J. N., and N. Cicek, 2017: Recovering agricultural nutrients (potassium and phosphorus) from biomass ash: A review of literature. Tech. Rep., Department of Biosystems Engineering, University of Manitoba, 11 pp., https://doi.org/10.13140/RG.2.2.24745.85605.

Adams, A. M., J. M. Prospero, and C. Zhang, 2012: *CALIPSO*-derived three-dimensional structure of aerosol over the Atlantic basin and adjacent continents. *J. Climate*, **25**, 6862–6879, https://doi.org/10.1175/JCLI-D-11-00672.1.

Akagi, S. K., R. J. Yokelson, C. Wiedinmyer, M. J. Alvarado, J. S. Reid, T., Karl, J. D. Crounse, and P. O. Wennberg, 2011: Emission factors for open and domestic biomass burning for use in atmospheric models, *Atmos. Chem. Phys.*, **11**, 4039–4072, https://doi.org/10.5194/acp-11-4039-2011.

Andreae, M. O., 1995: Climatic effects of changing atmospheric aerosol levels. *Future Climates of the World: A Modelling Perspective*, A. Henderson-Sellers, Ed., World Survey of Climatology, Vol., 16, Elsevier, 347–398, https://doi.org/10.1016/S0168-6321(06)80033-7.

Augustin-Bauditz, S., H. Wex, S. Kanter, M. Ebert, D. Niedermeier, F. Stolz, A. Prager, and F. Stratmann, 2014: The immersion mode ice nucleation behavior of mineral dusts: A comparison of different pure and surface modified dusts. *Geophys. Res. Lett.*, **41**, 7375–7382, https://doi.org/10.1002/2014GL061317.

Bozlaker, A., J. M. Prospero, J. Price, and S. Chellam, 2018: Linking Barbados mineral dust aerosols to North African sources using elemental composition and radiogenic Sr, Nd, and Pb isotope signatures. *J. Geophys. Res. Atmos.*, **123**, 1384–1400, https://doi.org/10.1002/2017JD027505.

——, ——, ——, and ——, 2019: Identifying and quantifying the impacts of advected North African dust on the concentration and composition of airborne fine particulate matter in Houston and Galveston, Texas. *J. Geophys. Res. Atmos.*, **124**, 12 282–12 300, https://doi.org/10.1029/2019JD030792.

Carlson, T. N., and J. M. Prospero, 1972: The large-scale movement of Saharan Air outbreaks over the northern equatorial Atlantic. *J. Appl. Meteor.*, **11**, 283–297, https://doi.org/10.1175/1520-0450(1972)0112.0.CO;2.

Chen, Q., and Coauthors, 2009: Mass spectral characterization of submicron biogenic organic particles in the Amazon basin. *Geophys. Res. Lett.*, **36**, L20806, https://doi.org/10.1029/2009GL039880.

Córdoba, F., 2019: Caracterización del aerosol atmosférico en la Península de Yucatán y su potencial influencia en los patrones de precipitación regionales. M.Sc. thesis, Centro de Ciencias de la Atmosfera, Universidad Nacional Autónoma de México, 159 pp., http://132.248.9.41:8880/jspui/handle/DGB_UNAM/TES01000789476.

——, and Coauthors, 2021: Measurement report: Ice nucleating abilities of biomass burning, African dust, and sea spray aerosol particles over the Yucatán Peninsula. *Atmos. Chem. Phys.*, **21**, 4453–4470, https://doi.org/10.5194/acp-21-4453-2021.

Creamean, J. M., and Coauthors, 2013: Dust and biological aerosols from the Sahara and Asia influence precipitation in the western U.S. *Science*, **339**, 1572–1578, https://doi.org/10.1126/science.1227279.

Das, R., A. Evans, and D. Lawrence, 2013: Contributions of long-distance dust transport to atmospheric P inputs in the Yucatan Peninsula. *Global Biogeochem. Cycles*, **27**, 167–175, https://doi.org/10.1029/2012GB004420.

DeMott, P. J., K. Sassen, M. R. Poellot, D. Baumgardner, D. C. Rogers, S. D. Brooks, A. J. Prenni, and S. M. Kreidenweis, 2003: African dust aerosols as atmospheric ice nuclei. *Geophys. Res. Lett.*, **30**, 1732, https://doi.org/10.1029/2003GL017410.

——, and Coauthors, 2015: Integrating laboratory and field data to quantify the immersion freezing ice nucleation activity of mineral dust particles. *Atmos. Chem. Phys.*, **15**, 393–409, https://doi.org/10.5194/acp-15-393-2015.

Després, V. R., A. Huffman, J. Burrows, C. Hoose, A. S. Safatov, G. Buryak, and J. Fröhlich-Nowoisky, 2012: Primary biological aerosol particles in the atmosphere: A review. *Tellus*, **64B**, 15598, https://doi.org/10.3402/tellusb.v64i0.15598.

Diaz-Esteban, Y., and G. B. Raga, 2017: Weather regimes associated with summer rainfall variability over southern Mexico. *Int. J. Climatol.*, **38**, 169–186, https://doi.org/10.1002/joc.5168.

——, and ——, 2019: Observational evidence of the transition from shallow to deep convection in the western Caribbean trade winds. *Atmosphere*, **10**, 700, https://doi.org/10.3390/atmos10110700.

Dominguez-Martinez, R., and D. A. Rodriguez, 2008: Forest fires in Mexico and Central America. Proceedings of the Second International Symposium on Fire Economics, Planning, and Policy: A global view, USDA Forest Service General Tech. Rep. PSW-GTR-208, 709–720, www.fs.fed.us/psw/publications/documents/psw_gtr208en/psw_gtr208en_709-720_dominquez.pdf.

Espinosa, A. A., J. Reyes-Herrera, J. Miranda, F. Mercado, M. A. Veytia, M. Cuautle, and J. I. Cruz, 2012: Development of an X-ray fluorescence spectrometer for environmental science applications. *Instrum. Sci. Technol.*, **40**, 603–617, https://doi.org/10.1080/10739149.2012.693560.

Evan, A. T., and S. Mukhopadhyay, 2010: African dust over the northern tropical Atlantic: 1955–2008. *J. Appl. Meteor. Climatol.*, **49**, 2213–2229, https://doi.org/10.1175/2010JAMC2485.1.

Feingold, G., H. Jiang, and J. Y. Harrington, 2005: On smoke suppression of clouds in Amazonia. *Geophys. Res. Lett.*, **32**, L02804, https://doi.org/10.1029/2004GL021369.

Forster, P., and Coauthors, 2007. Changes in atmospheric constituents and in radiative forcing. *Climate Change 2007: The Physical Science Basis*, S. Solomon et al., Eds., Cambridge University Press, 129–234.

Ganor, E., and Y. Mamane, 1982: Transport of Saharan dust across the eastern Mediterranean. *Atmos. Environ.*, **16**, 581–587, https://doi.org/10.1016/0004-6981(82)90167-6.

Giglio, L., 2007: Characterization of the tropical diurnal fire cycle using VIRS and MODIS observations. *Remote Sens. Environ.*, **108**, 407–421, https://doi.org/10.1016/j.rse.2006.11.018.

——, I. Csiszar, and C. O. Justice, 2006: Global distribution and seasonality of active fires as observed with the Terra and Aqua Moderate Resolution Imaging Spectroradiometer (MODIS) sensors. *J. Geophys. Res. Biogeosci.*, **111**, G02016, https://doi.org/10.1029/2005JG000142.

Griffin, D. W., 2007: Atmospheric movement of microorganisms in clouds of desert dust and implications for human health. *Clin. Microbiol. Rev.*, **20**, 459–477, https://doi.org/10.1128/CMR.00039-06.

Guerzoni, S., E. Molinaroli, and R. Chester, 1997: Saharan dust inputs to the western Mediterranean Sea: depositional patterns, geochemistry and sedimentological implications. *Deep-Sea Res. II*, **44**, 631–654, https://doi.org/10.1016/S0967-0645(96)00096-3.

Huang, J. F., C. D. Zhang, and J. M. Prospero, 2010: African dust outbreaks: A satellite perspective of temporal and spatial variability over the tropical Atlantic Ocean. *J. Geophys. Res.*, **115**, D05202, https://doi.org/10.1029/2009JD012516.

INEGI, 2015: Principales resultados de la Encuesta Intercensal 2015: Yucatán. Instituto Nacional de Estadística y Geografía, 96 pp., www.inegi.org.mx/contenidos/productos/prod_serv/contenidos/espanol/bvinegi/productos/nueva_estruc/inter_censal/estados2015/702825080051.pdf.

Kandler, K., and Coauthors, 2011: Ground-based off-line aerosol measurements at Praia, Cape Verde, during the Saharan Mineral Dust Experiment: Microphysical properties and mineralogy. *Tellus*, **63**, 459–474, https://doi.org/10.1111/j.1600-0889.2011.00546.x.

——, K. Schneiders, M. Ebert, M. Hartmann, S. Weinbruch, M. Prass, and C. Pöhlker, 2018: Composition and mixing state of atmospheric aerosols determined by electron microscopy: Method development and application to aged Saharan dust deposition in the Caribbean boundary layer. *Atmos. Chem. Phys.*, **18**, 13 429–13 455, https://doi.org/10.5194/acp-18-13429-2018.

Kanji, Z. A., L. A. Ladino, H. Wex, Y. Boose, D. J. Cziczo, M. Kohn, and M. Kramer, 2017: Overview of ice nucleating particles. *Ice Formation and Evolution in Clouds and Precipitation: Measurement and Modeling Challenges*, *Meteor. Monogr.*, No. 58, Amer. Meteor. Soc., 1.1–1.33, https://doi.org/10.1175/AMSMONOGRAPHS-D-16-0006.1.

Karnauskas, K. B., R. Seager, A. Giannini, and A. J. Busalacchi, 2013: A simple mechanism for the climatological midsummer drought along the Pacific coast

of Central America. *Atmósfera*, **26**, 261–281, https://doi.org/10.1016/S0187-6236(13)71075-0.

Koren, I., Y. J. Kaufman, L. Remer, and J. V. Martins, 2004: Measurement of the effect of Amazon smoke on inhibition of cloud formation. *Science*, **303**, 1342–1345, https://doi.org/10.1126/science.1089424.

Korontzi, S., J. McCarty, T. Loboda, S. Kumar, and C. Justice, 2006: Global distribution of agricultural fires in croplands from 3 years of Moderate Resolution Imaging Spectroradiometer (MODIS) data. *Global Biogeochem. Cycles*, **20**, GB2021, https://doi.org/10.1029/2005GB002529.

Ladino, L. A., and Coauthors, 2019: Ice nucleating particles in a coastal tropical site. *Atmos. Chem. Phys.*, **19**, 6147–6165, https://doi.org/10.5194/acp-19-6147-2019.

——, and Coauthors, 2021: The UNAM-Droplet Freezing Assay: An evaluation of the ice nucleating capacity of the sea-surface microlayer and surface mixed layer in tropical and subpolar waters. *Atmósfera*, https://doi.org/10.20937/ATM.52938, in press.

Lau, K., and H. Wu, 2003: Warm rain processes over tropical oceans and climate implications. *Geophys. Res. Lett.*, **30**, 2290, https://doi.org/10.1029/2003GL018567.

Linke, C., O. Möhler, A. Veres, Á. Mohácsi, Z. Bozóki, G. Szabó, and M. Schnaiter, 2006: Optical properties and mineralogical composition of different Saharan mineral dust samples: A laboratory study. *Atmos. Chem. Phys.*, **6**, 3315–3323, https://doi.org/10.5194/acp-6-3315-2006.

Liu, D., and Coauthors, 2018: Aircraft and ground measurements of dust aerosols over the west African coast in summer 2015 during ICE-D and AER-D. *Atmos. Chem. Phys.*, **18**, 3817–3838, https://doi.org/10.5194/acp-18-3817-2018.

Liu, Y., and Y. Xue, 2020: Expansion of the Sahara Desert and shrinking of frozen land of the Arctic. *Sci. Rep.*, **10**, 4109, https://doi.org/10.1038/s41598-020-61085-0.

Magaña, V., J. A. Amador, and S. Medina, 1999: The midsummer drought over Mexico and central America. *J. Climate*, **12**, 1577–1588, https://doi.org/10.1175/1520-0442(1999)0122.0.CO;2.

Maki, L. R., and K. J. Willoughby, 1978: Bacteria as biogenic sources of freezing nuclei. *J. Appl. Meteor.*, **17**, 1049–1053, https://doi.org/10.1175/1520-0450(1978)0172.0.CO;2.

Marsden, N. A., and Coauthors, 2019: Mineralogy and mixing state of north African mineral dust by online single-particle mass spectrometry. *Atmos. Chem. Phys.*, **19**, 2259–2281, https://doi.org/10.5194/acp-19-2259-2019.

Mayol-Bracero, O. L., and Coauthors, 2020: "Godzilla" African dust event of June 2020: Impacts of air quality in the greater Caribbean Basin, the Gulf of Mexico and the United States. *AGU Fall Meeting*, Online, Amer. Geophys. Union, Abstract A016-02.

Mukhopadhyay, S., and P. Kreycik, 2008: Dust generation and drought patterns in Africa from helium-4 in a modern Cape Verde coral. *Geophys. Res. Lett.*, **35**, L20820, https://doi.org/10.1029/2008GL035722.

Muñoz-Salazar, J., G. B. Raga, J. Yakobi-Hancock, J. S. Kim, D. Rosas, L. Caudillo, H. Alvarez-Ospina, and L. A. Ladino, 2020: Ultrafine aerosol particles in the western Caribbean: A first case study in Merida. *Atmos. Pollut. Res.*, **11**, 1767–1775, https://doi.org/10.1016/j.apr.2020.07.008.

Peppler, R. A., and Coauthors, 1999: Identification and analysis of the 1998 Central American smoke event at the ARM SGP Cart site. *Proc. of the Ninth ARM Science Team Meeting*, San Antonio, TX, U.S. Dept. of Energy, 16 pp., https://armweb0-stg.ornl.gov/publications/proceedings/conf09/extended_abs/peppler_ra.pdf.

Perdigón-Morales, J., R. Romero-Centeno, B. S. Barrett, and P. Ordoñez, 2019: Intraseasonal variability of summer precipitation in Mexico: MJO influence on the midsummer drought. *J. Climate*, **32**, 2313–2327, https://doi.org/10.1175/JCLI-D-18-0425.1.

Ponce-Caballero, C., M. Gamboa-Marrufo, M. López-Pacheco, I. Cerón-Palma, C. Quintal- Franco, G. Giácoman-Vallejos, and J.H. Loría-Arcila, 2013: Seasonal variation of airborne fungal propagules indoor and outdoor of domestic environments in Mérida, Mexico. *Atmósfera*, **26**, 369–377, https://doi.org/10.1016/S0187-6236(13)71083-X.

Price, H. C., and Coauthors, 2018: Atmospheric ice-nucleating particles in the dusty tropical Atlantic. *J. Geophys Res. Atmos.*, **123**, 2175–2193, https://doi.org/10.1002/2017JD027560.

Prospero, J. M., and T. N. Carson, 1972: Vertical and aerial distribution of Saharan Dust over the western equatorial North Atlantic Ocean. J. Geophys. Res., **77**, 5255–5265, https://doi.org/10.1029/JC077i027p05255.

——, and O. Mayol-Bracero, 2013: Understanding the transport and impact of African Dust on the Caribbean Basin. *Bull. Amer. Meteor. Soc.*, **94**, 1329–1337, https://doi.org/10.1175/BAMS-D-12-00142.1.

——, W. M. Landing, and M. Schulz, 2010: African dust deposition to Florida: Temporal and spatial variability and comparisons to models. *J. Geophys. Res.*, **115**, D13304, https://doi.org/10.1029/2009JD012773.

Querol, X., and Coauthors, 2019: Monitoring the impact of desert dust outbreaks for air quality for health studies. *Environ. Int.*, **130**, 104867, https://doi.org/10.1016/j.envint.2019.05.061.

Raga, G. B., D. Baumgardner, and O. Mayol-Bracero, 2016: History of aerosol-cloud interactions derived from observations in mountaintop clouds in Puerto Rico. *Aerosol Air Qual. Res.*, **16**, 674–688, https://doi.org/10.4209/aaqr.2015.05.0359.

Ramírez-Romero, C., and Coauthors, 2021: African dust particles over the western Caribbean Part I: Impact on air quality over the Yucatan Peninsula. *Atmos. Chem. Phys.*, **21**, 239–253, https://doi.org/10.5194/acp-21-239-2021.

Ramírez-Romero, M. C., 2019: Influencia del polvo mineral y la quema de biomasa en la formación de nubes mixtas en la Península de Yucatán. M.Sc. thesis, Centro de Ciencias de la Atmosfera, Universidad Nacional Autónoma de México, 177 pp., http://132.248.9.41:8880/jspui/handle/DGB_UNAM/TES01000794524.

Rios, B., and G. B. Raga, 2018: Spatio-temporal distribution of burned areas by ecoregions in Mexico and Central America. *Int. J. Remote Sens.*, **39**, 949–970, https://doi.org/10.1080/01431161.2017.1392641.

——, and ——, 2019: Smoke emissions from agricultural fires in Mexico and Central America. *J. Appl. Remote Sens.*, **13**, 036509, https://doi.org/10.1117/1.JRS.13.036509.

Rodríguez-Gómez, C., and Coauthors, 2020: Characterization of culturable airborne microorganisms in the Yucatan Peninsula. *Atmos. Environ.*, **223**, 117183, https://doi.org/10.1016/j.atmosenv.2019.117183.

Rogers, C. F., J. G. Hudson, B. Zielinska, R. L. Tanner, J. Hallett, and J. G. Watson, 1991: Cloud condensation nuclei from biomass burning. *Global Biomass Burning: Atmospheric, Climatic and Biospheric Implications*, J. S. Levine, Ed., MIT Press, 431–438.

SEDESOL, 2013: General data. Secretaría de Desarrollo Social: Cédulas de Información Municipal (SCIM), www.microrregiones.gob.mx/zap/datGenerales.aspx?entra=pdzp&ent=31&mun=038.

Trapp, J. M., J. F. Millero, and J. M. Prospero, 2010: Temporal variability of the elemental composition of African dust measured in trade wind aerosols at Barbados and Miami. *Mar. Chem.*, **120**, 71–82, https://doi.org/10.1016/j.marchem.2008.10.004.

Trujano-Jiménez, F., B. Ríos, A. Jaramillo, L. A. Ladino, and G. B. Raga, 2021: The impact of biomass burning emissions on protected natural areas in central and southern Mexico. *Environ. Sci. Pollut. Res. Int.*, **28**, 17 275–17 289, https://doi.org/10.1007/s11356-020-12095-y.

Twohy, C. H., and Coauthors, 2009: Saharan dust particles nucleate droplets in eastern Atlantic clouds. *Geophys. Res. Lett.*, **36**, L01807, https://doi.org/10.1029/2008GL035846.

van der Werf, G. R., J. T. Randerson, L. Giglio, G. J. Collatz, P. S. Kasibhatla, and A. F. Arellano Jr., 2006: Interannual variability in global biomass burning emissions from 1997 to 2004. *Atmos. Chem. Phys.*, **6**, 3423–3441, https://doi.org/10.5194/acp-6-3423-2006.

Weinzierl, B., et al., 2017: The Saharan Aerosol Long-Range Transport and Aerosol-Cloud-Interaction Experiment: Overview and selected highlights. *Bull. Amer. Meteor. Soc.*, **98**, 1427–1451, https://doi.org/10.1175/BAMS-D-15-00142.1.

Wex, H., and Coauthors, 2015: Intercomparing different devices for the investigation of ice nucleating particles using Snomax® as test substance. *Atmos. Chem. Phys.*, **15**, 1463–1485, https://doi.org/10.5194/acp-15-1463-2015.

Wiedinmyer, C., B. Quayle, C. Geron, A. Belote, D. McKenzie, X. Zhang, S. O'Neill, and K. K. Wynne, 2006: Estimating emissions from fires in North America for air quality modeling. *Atmos. Environ.*, **40**, 3419–3432, https://doi.org/10.1016/j.atmosenv.2006.02.010.

Wilson, T. W., and Coauthors, 2015: A marine biogenic source of atmospheric ice-nucleating particles. *Nature*, **525**, 234–238, https://doi.org/10.1038/nature14986.

Yakobi-Hancock, J. D., L. A. Ladino, and J. P. Abbatt, 2014: Review of recent developments and shortcomings in the characterization of potential atmospheric ice nuclei: Focus on the tropics. *Revista de Ciencias*, **17**, 15–34, https://doi.org/10.25100/rc.v17i3.476.

Yankofsky, S., Z. Levin, T. Bertold, and N. Sandlerman, 1981: Some basic characteristics of bacterial freezing nuclei. *J. Appl. Meteor.*, **20**, 1013–1019, https://doi.org/10.1175/1520-0450(1981)0202.0.CO;2.

Yokelson, R. J., and Coauthors, 2009: Emissions from biomass burning in the Yucatan. *Atmos. Chem. Phys.*, **9**, 5785–5812, https://doi.org/10.5194/acp-9-5785-2009.

——, and Coauthors, 2011: Trace gas and particle emissions from open biomass burning in Mexico. *Atmos. Chem. Phys.*, **11**, 6787–6808, https://doi.org/10.5194/acp-11-6787-2011.

Zhang, H., G. M. McFarquhar, S. M. Saleeby, and W. R. Cotton, 2007: Impacts of Saharan dust as CCN on the evolution of an idealized tropical cyclone. *Geophys. Res. Lett.*, **34**, L14812, https://doi.org/10.1029/2007GL029876.